IEEE Access
Multidisciplinary | Rapid Review | Open Access Journal

Digital Object Identifier

EEG Classification of Forearm Movement Imagery Using A Hierarchical Flow Convolutional Neural Network

JI-HOON JEONG[1], BYEONG-HOO LEE[1], DAE-HYEOK LEE[1], YONG-DEOK YUN[1], AND SEONG-WHAN LEE[2], (FELLOW, IEEE)

[1]Department of Brain and Cognitive Engineering, Korea University, Anam-dong, Seongbuk-ku, Seoul 02841, South Korea (e-mail: jh_jeong@korea.ac.kr, bh_lee@korea.ac.kr, lee_dh@korea.ac.kr, yd_yun@korea.ac.kr.)
[2]Department of Artificial Intelligence, Korea University, Anam-dong, Seongbuk-ku, Seoul 02841, South Korea

Corresponding author: Seong-Whan Lee (e-mail: sw.lee@korea.ac.kr).

This work was partly supported by Institute of Information & Communications Technology Planning & Evaluation (IITP) grant funded by the Korea government (No. 2017-0-00432, Development of Non-Invasive Integrated BCI SW Platform to Control Home Appliances and External Devices by User's Thought via AR/VR Interface), partly supported by IITP grant funded by the Korea government (No. 2017-0-00451, Development of BCI based Brain and Cognitive Computing Technology for Recognizing User's Intentions using Deep Learning), and partly supported by IITP grant funded by the Korea government (No. 2019-0-00079, Department of Artificial Intelligence, Korea University).

ABSTRACT Recent advances in brain-computer interface (BCI) techniques have led to increasingly refined interactions between users and external devices. Accurately decoding kinematic information from brain signals is one of the main challenges encountered in the control of human-like robots. In particular, although the forearm of an upper extremity is frequently used in daily life for high-level tasks, only few studies addressed decoding of the forearm movement. In this study, we focus on the classification of forearm movements according to elaborated rotation angles using electroencephalogram (EEG) signals. To this end, we propose a hierarchical flow convolutional neural network (HF-CNN) model for robust classification. We evaluate the proposed model not only with our experimental dataset but also with a public dataset (BNCI Horizon 2020). The grand-average classification accuracies of three rotation angles yield 0.73 ($\pm$0.04) for the motor execution (ME) task and 0.65 ($\pm$0.09) for the motor imagery (MI) task across ten subjects in our experimental dataset. Further, in the public dataset, the grand-averaged classification accuracies were 0.52 ($\pm$0.03) for ME and 0.51 ($\pm$0.04) for MI tasks across fifteen subjects. Our experimental results demonstrate the possibility of decoding complex kinematics information using EEG signals. This study will contribute to the development of a brain-controlled robotic arm system capable of performing high-level tasks.

INDEX TERMS Brain-computer interface (BCI), Electroencephalogram (EEG), Convolutional neural network (CNN), Forearm motor execution and motor imagery

I. INTRODUCTION

BRAIN-COMPUTER interface (BCI) has been developed as an approach to assist patients suffering from a severe nerve injury. The BCI is used to recognize user intention to enable interaction between humans and external devices using brain signals. Non-invasive BCI is particularly fascinating as no surgical implant is needed [1]–[3]. It has been demonstrated to steadily establish communication between humans and various devices such as an exoskeleton [4], [5], a wheelchair [6], a speller [7]–[9], and a robotic arm [10]–[14]. The electroencephalogram (EEG) represents a type of brain signal that can be measured non-invasively by detecting electrical signals on the scalp with high temporal resolution and low cost, compared to other techniques. Presently, EEG signals are the most practical tools that measure fast dynamics in brain activity [2], [15]–[17].

EEG-based BCI has been investigated with respect to various paradigms, including exogenous and endogenous characteristics. In particular, motor imagery (MI) is used not only to rehabilitation (i.e., recovery of disabled movement function) for patients [18] but also to support the daily-life activities of healthy people [19]–[22]. The MI paradigm has advanced steadily, and the neurophysiological phenomena (e.g., event-related desynchronization and synchronization (ERD/ERS)) during motor execution (ME) are observed when MI is performed. ERD/ERS rhythms are identified from the mu-band

(8–12 Hz) and the beta-band (13–30 Hz) across the primary sensorimotor area [23]. However, the ERD/ERS pattern can detect differences in band-specific signal patterns and the location of the occurrence depending on the individual characteristics [24]. Hence, decoding the user intention from EEG signals based on MI for high-level tasks represents one of the challenges [25]–[29].

A few groups developed the advanced decoding methods for the single upper extremity movement using EEG signals [28], [30]–[33]. Meng et al. [11] examined the possibility of using non-invasive motor imagination-based BCI for control of a robotic arm that executes reach-and-automatic-grasp tasks in 3D plane. Their experimental design effectively reduced the number of degrees of freedom. Schwarz et al. [27] categorized hand motions for various types of objects. Their study demonstrated the capability to discriminate three reach-and-grasp actions prominent in people's everyday use using non-invasive BCI. Shiman et al. [30] decoded the upper extremity reaching movements in various directions using a robotic exoskeleton on a horizontal 2D plane. Edelman et al. [31] examined the separability of MI tasks involving four different manipulations of the right hand (i.e., flexion, extension, supination, and pronation) using an EEG source imaging method. Úbeda et al. [34] assessed the feasibility of decoding upper-limb kinematics from EEG signals in center-out reaching tasks during passive and active movements. They employed linear regression to decode upper-limb kinematics from EEG signals. Li et al. [33] proposed a kind of classification strategy using not only EEG signals but also surface electromyogram (sEMG) signals combination. They classified a variety of upper extremity movements such as hand open/close, wrist pronation/supination. The classification performance achieved by the fusion of sEMG and EEG signals was significantly better than that obtained by a single signal source of either sEMG or EEG across all subjects. In this study, we focused on user intention decoding using a single upper extremity for high-level tasks. To the best of our knowledge, this is the first effort to categorize forearm movements and imageries according to various rotation angles using EEG signals in non-invasive BCI studies.

Furthermore, we adopted a deep learning approach for decoding complex ME and MI tasks using only EEG signals. Recent BCI advances have been applied to deep learning techniques which could generate a new signal feature representation and architecture training [35], [36]. Therefore, this approach provided further performance improvement for robust decoding of the intention robustly. For example, Lu et al. [37] proposed a novel deep learning model based on a restricted Boltzmann machine (RBM) for MI classification. Frequency-domain representations of EEG signals obtained through the fast Fourier transform and wavelet package decomposition are obtained to train three RBMs. Zhang et al. [38] proposed a novel deep learning approach combined with data augmentation for EEG classification. They utilized the empirical mode decomposition on EEG frames and mixed their intrinsic mode functions to create new artificial

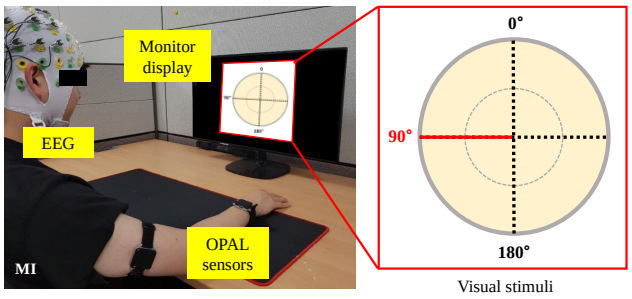

FIGURE1: Experimental environment for EEG data acquisition.

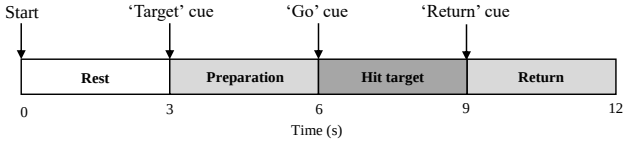

FIGURE2: Experimental paradigm in a single-trial.

EEG frames. Further, they proposed binary neural networks (i.e., convolutional and wavelet neural networks) to train the weights and allocate two classes of motor-imagery signals. Wang et al. [39] developed an LSTM-based framework to extract essential features of time-dependent EEG signals. The channel weighting technique is applied to make the EEG signal representation more concise. The channel weighting coefficients were automatically optimized with other network parameters of the LSTM network.

In this study, we designed an experimental environment to collect EEG signals corresponding to $0\,^{\circ}$, $90\,^{\circ}$, and $180\,^{\circ}$ angles of the forearm movement. We proposed a novel hierarchical flow convolutional neural network (HF-CNN) model for EEG classification. We evaluated the proposed model with not only our experimental dataset but also the public dataset related to forearm movements. Through the verification, we confirmed the feasibility of EEG classification for high-level tasks using a single upper extremity. This possibility demonstrates intuitive decoding of the user intention for BCI-based robotic arm/prosthesis control and the neuro-rehabilitation of stroke patients.

II. METHODS

A. DATA ACQUISITION

1) PARTICIPANTS

Ten subjects (ten males, all right-handed, age: 24–31 years) were recruited in our experiment. None of the subjects had a history of psychiatric or neurological disorders. This study was approved by the Institutional Review Board (IRB) at the Korea University [1040548-KU-17-172-A-21], and all subjects provided informed consent according to the Declaration of Helsinki prior to the experiments.

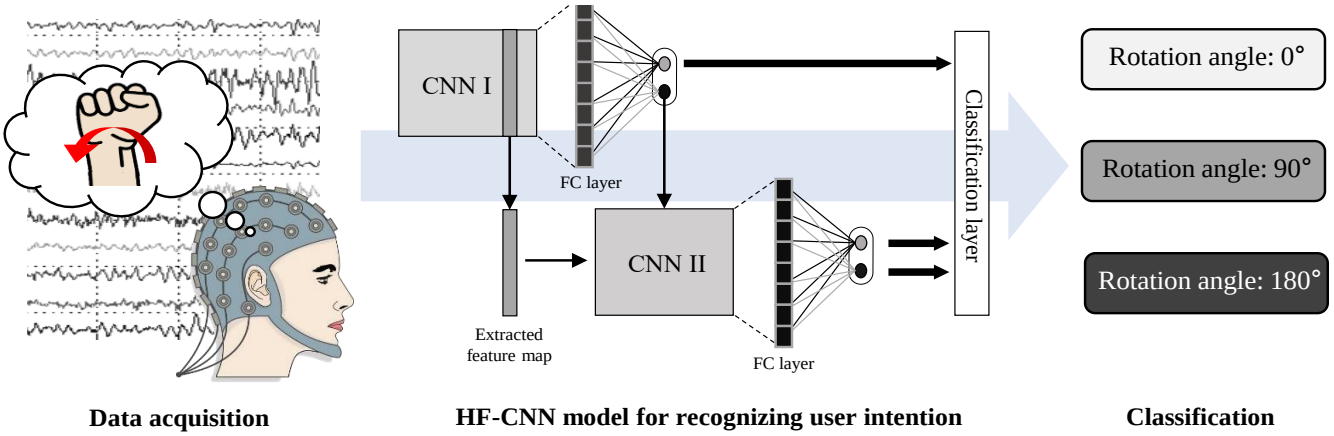

FIGURE3: Overview of the proposed HF-CNN model for classifying the forearm rotation from EEG signals.

2) EXPERIMENTAL SETUP

Fig. 1 shows the experimental environment for measuring EEG signals and kinematic data used in the experiment. The subjects sit in a comfortable chair at a monitor viewing distance of approximately 60 cm at a desk. Visual stimuli were presented on the monitor display as forearm rotation angles. The EEG signals were measured using 32 EEG channels according to the international 10-20 systems. The ground and reference electrodes were placed at AFz and FCz, respectively. We selected 20 EEG channels near the primary/supplementary motor cortices to avoid artifacts related to facial or eyeball movements (i.e., FC5, FC3, FC1, FCz, FC2, FC4, FC6, C5, C3, C1, Cz, C2, C4, C6, CP5, CP3, CP1, CPz, CP2, CP4, and CP6) [12], [40], [41]. Those channels located in central brain area were activated when the subjects executed movements and imagined their muscle movement [23]. A sampling rate of 100 Hz and a notch filter frequency rate of 60 Hz were applied to reduce the DC power supply noise. The impedance of all electrodes was maintained below 10 kΩ.

The kinematic information of forearm rotation angles was collected by two motion sensors (OPAL, APDM Inc., Canada). The sensors were strapped to the front of the right forearm and outside of the right upper extremity, as shown in Fig. 1. We obtained the angular position and velocity using an accelerometer and gyroscope information obtained through the OPAL sensor [42]. Then, we confirmed the kinematic information to verify whether the forearm movement or not according to the ME and MI tasks. The kinematic information could show how well the subject performed the experimental protocol for each task and collected high-quality data. For example, if the subject were asked to perform the MI task, the kinematic information could not show any activation of kinematic information owing to no movement at that time. Meanwhile, in the ME tasks, the kinematic information could show some activation while the subject was performing an upper extremity movement task.

3) EXPERIMENTAL PARADIGM

Fig. 2 illustrates the experimental paradigm for EEG data acquisition. The experiment comprised ME and MI task sessions, each containing 150 trials (50 trials per target angle). A single-trial consisted of four phases, namely 'rest', 'preparation', 'hit target', and 'return'. Each trial began with a rest phase that lasted three seconds. At this time, the subjects were asked to maintain the resting state with minimum body movement. In the preparation phase, after a beep sound, one of the target cues (0 °, 90 °, and 180 °) was presented by a red line to the subjects. After being shown the target angles, the subjects performed the ME task that corresponds to the target by rotating their forearm during 3 s, whereas in the MI task session, the imagined their forearm according to the target angles. During this period, they were asked to minimize eye blinking and head movement. After 3 s, the subjects returned their forearm to the 0 ° position in a procedure lasting 3 s.

B. PROPOSED METHOD

An overview of the classification for forearm movement and the imagery from EEG signals using the proposed model is depicted in Fig. 3. All data processing was carried out using the PyTorch library and MATLAB 2019a (MathWorks, USA) software with a high-performance computer. After the data acquisition, EEG data were preprocessed by a zero-phase second-order Butterworth bandpass filter with a cutoff frequency from 4 to 40 Hz [43]. To obtain clear EEG data, we removed the contamination factors using an independent component analysis (ICA) algorithm which is commonly used. The contaminated ICs that had similar patterns of the Fp1 or Fp2 channels with respect to eye movement were automatically removed [44], [45]. The filtered EEG data were segmented according to each rotation angle. We adopted a deep learning approach to decode high-level tasks using only EEG signals.

In this study, we propose the HF-CNN model as a classification method. CNN is a multi-layer neural network based on convolution. It decodes the user intention from EEG signals

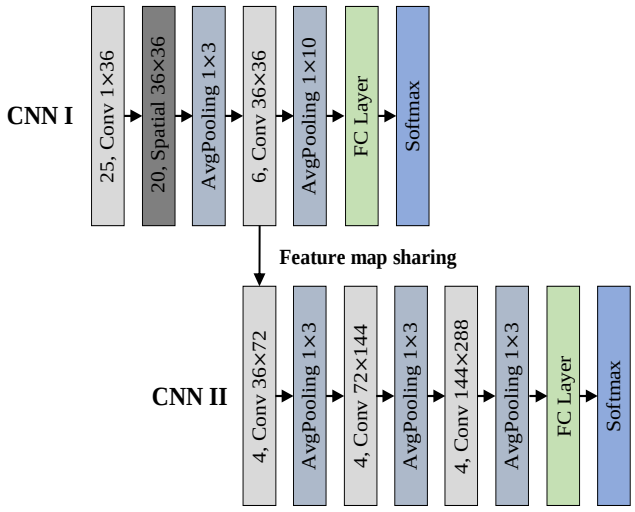

FIGURE4: Architecture of the proposed HF-CNN model.

[46], [47]. We designed the frame of CNN and adopted a hierarchical architecture to extract relevant features for multiple classifications. The HF-CNN was trained according to each subject because of the EEG uncertainty characteristics.

Initially, we randomly selected 80% of the trials as a training set and used the remaining 20% as a test set for classification [38]. The entire dataset included 150 trials comprising 50 trials per each class. Hence, the data from 120 trials (i.e., 40 trials×3 classes) were assigned for training, and the data from the remaining 30 trials were designated as test data. Fig. 4 shows the proposed HF-CNN architecture, composed of two main steps: CNN I for movement detection and CNN II for forearm rotation detection. CNN I and CNN II comprise three different layers: convolution, pooling, and the fully-connected layer. In the CNN I step, the dimensions of EEG signals as input data were 300×20 (*time*×*channel*). The convolutional layer was employed for the convolution over the entire input space to linearly transform it using a learnable kernel of 1×25 sizes to generate a receptive field from 4 to 40 Hz since sampling rate was 100 Hz. Subsequently, the data were processed through a 20×1 spatial filter to make the channel into a single channel. The average pooling layer, obtained after the spatial filter downsampled the convolution layer using a 1×3 kernel size, reduced the computational cost for multiple stacked layers. We assumed that classification between movement and resting state could be easily performed with low-level features. Therefore, CNN I performed only two convolutions and pooling. Followingly, a fully-connected (FC) layer flattened the features that were extracted through multiple layers. We applied an exponential linear unit (ELU) as the activation function. Using a cross-entropy loss function, the CNN architectures were trained to extract relevant features for classifying the input data (i.e., forearm rotation angle at 0 °).

The input data of CNN II comprised the features extracted by the last convolution layer of CNN I. The convolution was conducted with a 1×4 kernel size. The CNN II obtained relevant features for the forearm rotation classification as 90 ° or 180 ° through the three convolution blocks. Each softmax layer of CNN I and CNN II is connected for the end of classification process. Accordingly, if the classification result of CNN I is resting state, then the HF-CNN classified as resting state and the classification process would be terminated. Otherwise, a shared feature map is utilized in CNN II for further feature extraction and classification. In this case, the classification result of HF-CNN could be classified as the detailed rotation angle classification.

In this study, we modified each cross-entropy loss function of CNN I and CNN II to a single loss function owing to the hierarchical framework characteristics. To consider the number of classes for each CNN classifier, we applied the weighted loss function [51], [52]. In this experiment, both CNN I and CNN II have obtained the same number of classes. Therefore, we multiplied the ratio of 0.5 to each loss. The modified cross-entropy loss function is defined as:

$$\mathcal{L}oss(\mathcal{L}_1, \mathcal{L}_2) = 0.5 \times \mathcal{L}_1 + 0.5 \times \mathcal{L}_2 \tag{1}$$

Each loss term is a generalized cross-entropy loss term, defined as:

Algorithm 1: Training stage of HF-CNN

Input: Preprocessed EEG data $\{X, \Omega\}$
- $X = \{x_i\}_{i=1}^{D}$, $\{x_i\} \in \mathbb{R}^{N \times T}$: a set of EEG data for a single-trial, where D is total number of trials with N channels and T sample points
- $\Omega = \{O_i\}_{i=1}^{D}$: class labels, where $O_i \in \{0, 1, 2\}$ and D is total number of trials

Output: Trained model

Stage 1: Divide EEG data into a training set and test set at a ratio of 80:20
- X_{tr}: a training set of EEG data, Ω_{tr}: a label set of training data

Stage 2: Train CNN I
- The parameters of CNN I are initialized to random values and modify the class labels to binary values (rest and movement), defined as $\Omega_{tr,1} = \{O_{i,1}\}_{i=1}^{D}$ where $O_{i,1} \in \{0, 1\}$
- Store feature maps extracted in last convolution layer
- Generate loss value by calculating differences between CNN I output and class label $\Omega_{tr,1}$

Stage 3: Train CNN II
- The CNN II initializes its parameters and defines class labels as rotation at 90 ° and rotation at 180 °. $\Omega_{tr,2} = \{O_{i,2}\}_{i=1}^{D}$ where $O_{i,2} \in \{0, 1\}$
- Use stored feature maps to train CNN II.
- Generate loss value by calculating differences between CNN II output and class labels $\Omega_{tr,2}$
- Concatenate CNN I and CNN II outputs for class labels Ω

Stage 4: Fine-tune parameters
- Minimize loss values by tuning parameters of both CNN I and CNN II.

TABLE1: Classification accuracy of proposed and conventional methods for ME and MI tasks in DATASET I

Subjects	ME					MI				
	FBCSP [48]	ConvNet [49] (Shallow)	ConvNet [49] (Deep)	EEGNet [50]	HF-CNN	FBCSP [48]	ConvNet [49] (Shallow)	ConvNet [49] (Deep)	EEGNet [50]	HF-CNN
S01	0.35	0.70	0.60	0.70	0.77	0.35	0.60	0.53	0.53	0.60
S02	0.34	0.73	0.60	0.60	0.70	0.34	0.53	0.63	0.56	0.57
S03	0.35	0.73	0.60	0.63	0.77	0.35	0.63	0.57	0.60	0.63
S04	0.35	0.73	0.63	0.67	0.70	0.35	0.60	0.57	0.57	0.60
S05	0.38	0.63	0.73	0.60	0.67	0.36	0.53	0.53	0.63	0.70
S06	0.34	0.73	0.70	0.67	0.77	0.35	0.60	0.63	0.57	0.70
S07	0.35	0.73	0.67	0.60	0.70	0.35	0.73	0.67	0.60	0.70
S08	0.34	0.63	0.53	0.67	0.77	0.37	0.60	0.57	0.57	0.70
S09	0.35	0.77	0.63	0.63	0.73	0.34	0.56	0.63	0.56	0.67
S10	0.36	0.68	0.65	0.67	0.71	0.35	0.53	0.50	0.57	0.60
Average	0.35	0.71	0.63	0.64	0.73	0.35	0.57	0.56	0.57	0.65
Std.	±0.01	±0.04	±0.05	±0.03	±0.04	±0.01	±0.04	±0.04	±0.04	±0.09

$$\mathcal{L}_1 = -\sum_{c=1}^{2} y_1 \log \hat{y}_1 \tag{2}$$

$$\mathcal{L}_2 = -\sum_{c=1}^{N} y_2 \log \hat{y}_2 \tag{3}$$

$y_1$and y_2 are class labels of CNN I and CNN II, respectively; $\hat{y}_1$ and $\hat{y}_2$ are outputs of CNN I and CNN II. The hyper-parameter N depicts the number of forearm rotation classes. In this case, we set the value of N to 2.

In this manner, the proposed HF-CNN model classifies the forearm rotation angles ($0\,^\circ$, $90\,^\circ$, and $180\,^\circ$) from EEG signals obtained from each subject. We performed 300 iterations (epochs) for the model training process and saved the model weights that generate the least loss of the test data. The detailed training stage of the HF-CNN model is depicted in Algorithm 1.

C. PERFORMANCE EVALUATION

1) DATASET I: OUR EXPERIMENTAL DATASET

To fairly evaluate the proposed method, we applied 5-fold cross-validation and compared it with the existing methods for EEG decoding via an offline analysis. To this end, we evaluated the classification performance of existing methods (e.g., FBCSP [48], [53], ShallowConvNet [49], DeepConvNet [49], and EEGNet [50]) which were used for robust EEG classification.

As the deep learning approaches, the ConvNets [49] model is a robust CNN model employed to decode multi-classes in the MI dataset. The DeepConvNet model comprised four convolution-max-pooling blocks and used dropout layers with a 0.5 ratio to avoid overfitting problems. ShallowConvNet, inspired by the principle of FBCSP, included the first two layers (temporal convolution and spatial filter), thereby extracting the band power features [49]. Further, the EEGNet model, which is a compact CNN for EEG-based BCI for various paradigms (e.g., SMR and P300), comprises three different convolution layers to extract the representative features. The EEGNet exhibited a proficient classification performance compared to other existing methods [50]. In this study, using the test data, classification performances for forearm movement decoding were evaluated for each subject.

2) DATASET II: PUBLIC DATASET

Moreover, we validated the proposed HF-CNN model on the public dataset published by the BNCI Horizon 2020 project, which contains various upper extremity tasks, such as a forearm supination/pronation, elbow movement, hand grasping, and rest [54]. The dataset contained data acquired from fifteen subjects (six males and nine females, 22∼40 years) and acquired the EEG data using 61 channels. We classified the forearm supination class, forearm pronation class, and rest using the proposed HF-CNN model. The forearm movement classes are also correlated to the forearm rotation angle ($-90\,^\circ$, $0\,^\circ$, and $90\,^\circ$) similar to our experimentally obtained dataset. Hence, we conducted an evaluation of the proposed model to demonstrate its availability and efficiency.

III. EXPERIMENTAL RESULTS

Table 1 shows the classification accuracies of both the proposed model and existing methods for ME and MI tasks on the DATASET I. The proposed model exhibited the highest grand-average classification accuracy of 0.73 (±0.04) and 0.65 (±0.09) for both ME and MI tasks, respectively. The FBCSP with a regularized linear discriminant analysis (RLDA) [48], [53], one of the traditional machine learning methods for BCI decoding, exhibited the lowest classification accuracies of 0.35 (±0.01) for both tasks. This performance was similar to the chance level accuracy for the three-class problem (approximately 0.33). The deep learning approach showed outperformed the classification performance of the general machine learning method. In the ME task, EEGNet [50] and DeepConvNet [49] indicated grand-averaged accuracies of 0.63 (±0.04) and 0.64 (±0.03), respectively, for all subjects. The ShallowConvNet [49] achieved the highest classification accuracy of 0.71 (±0.04) among the deep learning methods. In the MI task, the deep learning method showed similar grand-average classification performance.

TABLE2: Classification accuracy of proposed and existing methods for ME and MI tasks in DATASET II

Subjects	ME					MI				
	FBCSP [48]	ConvNet [49] (Shallow)	ConvNet [49] (Deep)	EEGNet [50]	HF-CNN	FBCSP [48]	ConvNet [49] (Shallow)	ConvNet [49] (Deep)	EEGNet [50]	HF-CNN
S01	0.33	0.44	0.42	0.47	0.56	0.31	0.53	0.42	0.42	0.53
S02	0.34	0.47	0.53	0.50	0.50	0.33	0.48	0.39	0.44	0.51
S03	0.40	0.50	0.39	0.50	0.50	0.38	0.50	0.39	0.44	0.50
S04	0.36	0.50	0.42	0.50	0.53	0.37	0.46	0.44	0.50	0.50
S05	0.34	0.42	0.42	0.50	0.50	0.34	0.51	0.47	0.42	0.51
S06	0.36	0.56	0.47	0.47	0.50	0.36	0.47	0.44	0.47	0.47
S07	0.35	0.44	0.42	0.50	0.53	0.35	0.56	0.42	0.42	0.56
S08	0.37	0.50	0.42	0.50	0.50	0.34	0.47	0.44	0.44	0.47
S09	0.34	0.44	0.47	0.50	0.53	0.35	0.42	0.42	0.42	0.50
S10	0.37	0.42	0.44	0.50	0.47	0.31	0.56	0.44	0.50	0.56
S11	0.35	0.42	0.39	0.55	0.53	0.34	0.40	0.44	0.50	0.44
S12	0.36	0.42	0.42	0.50	0.50	0.36	0.44	0.47	0.42	0.50
S13	0.32	0.42	0.44	0.53	0.56	0.32	0.50	0.42	0.50	0.50
S14	0.36	0.50	0.47	0.56	0.53	0.34	0.47	0.42	0.39	0.47
S15	0.34	0.42	0.44	0.53	0.56	0.37	0.50	0.42	0.47	0.56
Average	0.35	0.45	0.43	0.50	0.52	0.34	0.48	0.42	0.45	0.51
Std.	±0.01	±0.04	±0.03	±0.02	±0.03	±0.02	±0.04	±0.02	±0.03	±0.04

Table 2 lists the classification accuracies for DATASET II (public dataset) using the proposed model and existing methods for ME and MI tasks. We conducted a three-class classification of forearm movements (i.e., forearm supination, forearm pronation, and rest). As depicted in Table 2, the proposed model outperformed the classification performance with accuracies of 0.52 (±0.03) for ME task and 0.51 (±0.04) for MI task, respectively, compared to the other methods.

The training accuracy for the HF-CNN for all subjects is shown in Fig. 5. In the model training phase, the classification performances are enhanced with an increasing number of epochs. The grand-average training accuracy indicated (black line) convergence within 100 epochs for both sessions. The grand-average training accuracies reached approximately 0.8 for all subjects. However, as depicted by the blue and green lines, the training performance exhibited the variation among the subjects. After completing the training process, the model is evaluated using the test dataset.

Fig. 6 shows the confusion matrix of the proposed model for multi-class classification on DATASET I and DATASET II. Each column of the confusion matrix represents the target class, whereas each row represents the predicted class (i.e., $0\,^\circ$, $90\,^\circ$, and $180\,^\circ$). In DATASET I, all true-positive values were higher than the true-negative values and the value of the false-negative for both ME and MI tasks. Further, for DATASET II, the configuration of the multi-class was composed of basic forearm movements, such as forearm pronation and forearm supination. As depicted in the confusion matrices, the true-positive of the rest class had the highest value among movement classes for all tasks (i.e., 0.83 for the ME and 0.70 for the MI). However, in the MI task, the proposed HF-CNN model confused the classification of forearm angles when the target class was $-90\,^\circ$, such that the model yielded the true positive as 0.50.

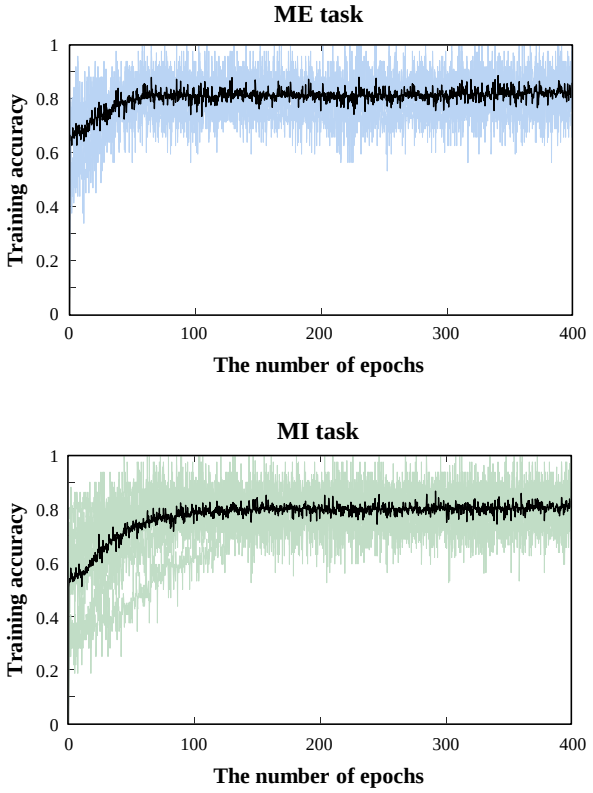

FIGURE5: Convergence curve of the proposed model training for both ME and MI tasks on DATASET I. Blue and green lines indicate curves of training accuracy according to each subject. Black line depicted depicts average training accuracy of model training across all subjects.

To verify the classification performance difference between the proposed model and existing methods, we conducted a statistical analysis employing the analysis of vari-

TABLE3: Results of significant performance difference using *t*-test for both datasets

DATASET I				DATASET II			
ME		MI		ME		MI	
Comparison group	*p*-value	Comparison group	*p*-value	Comparison group	*p*-value	Comparison group	*p*-value
FBCSP [48] vs. ShallowConvNet [49]	<0.01	FBCSP vs. ShallowConvNet	<0.01	FBCSP vs. ShallowConvNet	<0.01	FBCSP vs. ShallowConvNet	<0.01
FBCSP vs. DeepConvNet [49]	<0.01	FBCSP vs. DeepConvNet	<0.01	FBCSP vs. DeepConvNet	<0.01	FBCSP vs. DeepConvNet	<0.01
FBCSP vs. EEGNet [50]	<0.01	FBCSP vs. EEGNet	<0.01	FBCSP vs. EEGNet	<0.01	FBCSP vs. EEGNet	<0.01
FBCSP vs. HF-CNN	<0.01	FBCSP vs. HF-CNN	<0.01	FBCSP vs. HF-CNN	<0.01	FBCSP vs. HF-CNN	<0.01
ShallowConvNet vs. DeepConvNet	<0.01	ShallowConvNet vs. DeepConvNet	0.61	ShallowConvNet vs. DeepConvNet	0.07	ShallowConvNet vs. DeepConvNet	<0.01
ShallowConvNet vs. EEGNet	<0.01	ShallowConvNet vs. EEGNet	0.40	ShallowConvNet vs. EEGNet	<0.01	ShallowConvNet vs. EEGNet	<0.01
ShallowConvNet vs. HF-CNN	0.19	ShallowConvNet vs. HF-CNN	<0.01	ShallowConvNet vs. HF-CNN	<0.01	ShallowConvNet vs. HF-CNN	0.09
DeepConvNet vs. EEGNet	0.56	DeepConvNet vs. EEGNet	0.73	DeepConvNet vs. EEGNet	<0.01	DeepConvNet vs. EEGNet	0.09
DeepConvNet vs. HF-CNN	<0.01	DeepConvNet vs. HF-CNN	<0.01	DeepConvNet vs. HF-CNN	<0.01	DeepConvNet vs. HF-CNN	<0.01
EEGNet vs. HF-CNN	<0.01	EEGNet vs. HF-CNN	<0.01	EEGNet vs. HF-CNN	0.28	EEGNet vs. HF-CNN	<0.01

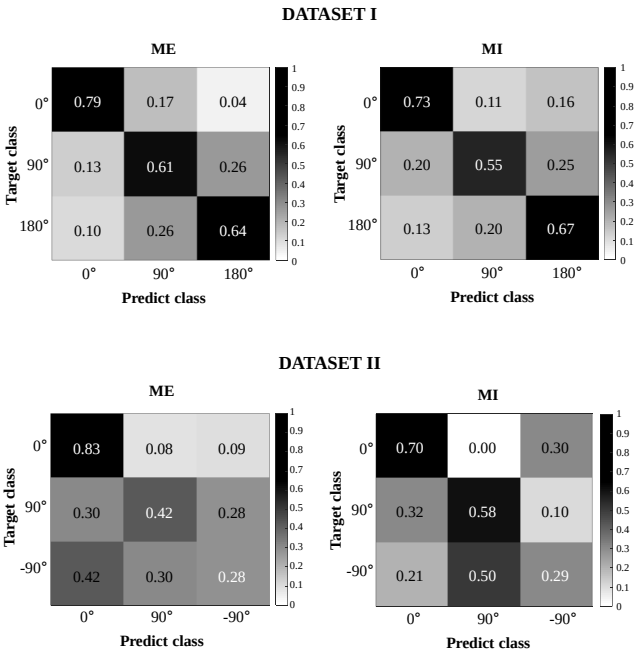

FIGURE6: Confusion matrices of grand-average classification results for all subjects according to DATASET I and DATASET II.

ance (ANOVA) with the Bonferroni correction. We performed multiple comparisons between groups using classification accuracy for fair statistical analysis for multi-group. The obtained *p*-values are given in Table 3. Most *p*-values are inferior to 0.01, which implies that the classification performance of the proposed model is statistically significant compared to the other methods. However, all obtained *p*-values of the general machine learning method (FBCSP) and deep learning approaches (ShallowConvNet, DeepConvNet, EEGNet, and HF-CNN) showed statistical significance (below 0.01). In our experimental dataset (DATASET I), there was no significant difference between the proposed model and ShallowConvNet for the ME task. The difference in the classification performance was approximately 0.2. For DATASET II, most groups exhibited a statistically significant difference, except ShallowConvNet vs. DeepConvNet and EEGNet vs. the proposed model with regard to the ME tasks. In the MI tasks, the performance difference between the proposed model and ShallowConvNet exhibited the lowest accuracy of approximately 0.3.

IV. DISCUSSION

In this study, we adopted a deep learning approach for recognizing user intention from EEG signals. We approached the complex upper-limb movement decoding that could possibly support BCI advances to perform high-level tasks using a robotic arm and neuro-prothesis. In particular, we focused on the classification of various angles of forearm rotations based on the HF-CNN. We acquired the EEG data for both the ME and MI tasks for ten subjects. We obtained the grand-average classification accuracies at 0.73 ($\pm$0.04) for ME and 0.65 ($\pm$0.09) for MI. Furthermore, we conducted the verification on a public dataset (DATASET II). The HF-CNN model exhibited the highest classification performance for the multi-class compared to the existing methods, as depicted in Table 2. However, the proposed model still requires improvement to achieve a further enhancement in its performance. In the MI task, HF-CNN exhibited a significant difference compared with other methods (Table 3), whereas in the ME task, the model remains with no statistical significance for the EEGNet model. This is because the ME task is induced by actual muscle activity, effectuating brain dynamics that are more distinct compared to the ones generated by imagination. Because EEG patterns for actual movement are prominent, we anticipated the methods using CNN architectures, including existing methods and HF-CNN, to be trained in a similar pattern for only ME task data.

In this paper, we proposed the hierarchical CNN architecture for reducing the workload of each singular CNN architecture. Generally, the parameters change in the network is one of the dramatic model performance improvements method, however, it has several limitations for the constrained environment such as using low-quality data and a

lack of the data [55]. Therefore, we adopted a hierarchical structure for classification instead of the parameter optimization method. Furthermore, CNN I and CNN II become more specialized to be classified as the 'movement or not' and '90° or 180°' angles in the model training. In this manner, the proposed model could serve as a novel model to solve complex MI decoding from EEG signals. However, the performance of HF-CNN is more dependent on CNN I since it adopted the principle of hierarchy. When CNN I classified improperly, the final results would be the wrong prediction regardless of the CNN II prediction. Hence, in order to overcome this limitation, we will need to modify the architecture that could reflect the error prediction.

Recent BCI advances adopted deep learning techniques, which already yielded a dramatically high performance in other research fields, such as computer vision and natural language processing [36]. In particular, a few studies applied the deep networks to various BCI paradigms using EEG signals such as mental state detection [56]–[59], emotion recognition [60], [61], intention decoding using steady-state visual evoked potentials [17], P300 [62], [63], and MI [35], [37]–[39], [49]. Several studies for MI decoding using deep learning approaches focused on enhancing decoding performance for basic multi-classes (e.g., left hand, right hand, and foot) using a public dataset [38], [39]. In contrast, in this study, we focused on practical MI tasks to consider applying real-world situations. The upper-limb movement decoding from EEG signals using a single-arm has recently developed as one of the challenging issues of the BCI [27], [30]. To the best of our knowledge, this is the novel study of complex forearm rotation classification using only EEG signals. Hence, this study could contribute to the advances of decoding for complex high-level tasks, including both ME and MI, based on deep learning approaches.

Furthermore, most deep learning architectures take considerable training time to achieve sufficient performance. The long calibration time is one of the critical problems in BCI advances, arising due to EEG non-stationary characteristics [64], [65]. Therefore, it is difficult to pre-train the deep learning model, as the EEG signals differ day by day. Additionally, in real-time BCI scenarios, the long training time for the model could affect the subjects' mental and physical state due to inattention [66]. In particular, when patients use the BCI system, considerable side effects could arise due to the long therapy phase. We designed the HF-CNN model to make possible its adoption in offline experiments as well as real-time scenarios. On average, the training time for each subject lasted approximately 20 s with a high-performance computer, which was configured with an Intel i7 CPU, a TITAN XP GPU, a 64-GB RAM, and 1-TB SSD. In this manner, the HF-CNN could contribute to a real-time BCI system by performing high-level tasks to support daily life and therapy. Therefore, we plan to evaluate the proposed model with real-time BCI scenarios such as pouring water or open a door using a robotic arm.

V. CONCLUSION AND FUTURE WORK

We presented the forearm rotation decoded from EEG signals based on the proposed deep learning approach. The proposed HF-CNN can classify complex MI tasks robustly owing to the hierarchical flow. We verified the model using both our experimental dataset and the public dataset. The results showed that the HF-CNN achieves prominent classification accuracy across both datasets. Therefore, the HF-CNN model is considered a promising tool for MI classification and BCI application. The model has the potential to perform high-level tasks, such as pouring water into a cup and opening a door using the EEG-based robotic arm or prosthesis.

In future work, we will modify the HF-CNN to enable the adoption of real-time BCI scenarios by improving classification performance. Hence, we will plan to apply more advanced machine learning algorithms such as the BCI adaptation method and boost artifacts rejections method. Moreover, we will develop the EEG-based robotic arm system based on the proposed model and test the developed system with regard to its ability to support daily work for healthy individuals and provide neuro-therapy for motor-disabled patients.

ACKNOWLEDGMENT

The authors thank Prof. C. Guan for the useful discussion on the data analysis and Mr. B.-W. Yu for the deep learning architecture design.

REFERENCES

[1] T. M. Vaughan, W. Heetderks, L. Trejo, W. Rymer, M. Weinrich, M. Moore, A. Kübler, B. Dobkin, N. Birbaumer, E. Donchin, E. Wolpaw, and J. Wolpaw, "Brain-computer interface technology: A review of the second international meeting," IEEE Trans. Neural Syst. Rehabil. Eng., vol. 11, no. 2, pp. 94–109, 2003.

[2] R. Abiri, S. Borhani, E. W. Sellers, Y. Jiang, and X. Zhao, "A comprehensive review of EEG-based brain-computer interface paradigms," J. Neural. Eng., vol. 16, no. 1, p. 011001, 2019.

[3] J. R. Wolpaw, N. Birbaumer, D. J. McFarland, G. Pfurtscheller, and T. M. Vaughan, "Brain–computer interfaces for communication and control," Clin. Neurophysiol., vol. 113, no. 6, pp. 767–791, 2002.

[4] Y. He, D. Eguren, J. M. Azorín, R. G. Grossman, T. P. Luu, and J. L. Contreras-Vidal, "Brain–machine interfaces for controlling lower-limb powered robotic systems," J. Neural. Eng., vol. 15, no. 2, p. 021004, 2018.

[5] N.-S. Kwak, K.-R. Müller, and S.-W. Lee, "A lower limb exoskeleton control system based on steady state visual evoked potentials," J. Neural. Eng., vol. 12, no. 5, p. 056009, 2015.

[6] K.-T. Kim, H.-I. Suk, and S.-W. Lee, "Commanding a brain-controlled wheelchair using steady-state somatosensory evoked potentials," IEEE Trans. Neural Syst. Rehabil. Eng., vol. 26, no. 3, pp. 654–665, 2018.

[7] M.-H. Lee, J. Williamson, D.-O. Won, S. Fazli, and S.-W. Lee, "A high performance spelling system based on EEG-EOG signals with visual feedback," IEEE Trans. Neural Syst. Rehabil. Eng., vol. 26, no. 7, pp. 1443–1459, 2018.

[8] T. Kaufmann and A. Kübler, "Beyond maximum speed—a novel two-stimulus paradigm for brain–computer interfaces based on event-related potentials (P300-BCI)," J. Neural Eng., vol. 11, no. 5, p. 056004, 2014.

[9] D.-O. Won, H.-J. Hwang, S. Dähne, K.-R. Müller, and S.-W. Lee, "Effect of higher frequency on the classification of steady-state visual evoked potentials," J. Neural Eng., vol. 13, no. 1, p. 016014, 2015.

[10] C. I. Penaloza and S. Nishio, "BMI control of a third arm for multitasking," Sci. Robot., vol. 3, no. 20, p. eaat1228, 2018.

[11] J. Meng, S. Zhang, A. Bekyo, J. Olsoe, B. Baxter, and B. He, "Noninvasive electroencephalogram based control of a robotic arm for reach and grasp tasks," Sci. Rep., vol. 6, p. 38565, 2016.

[12] J.-H. Jeong, K.-H. Shim, D.-J. Kim, and S.-W. Lee, "Brain-controlled robotic arm system based on multi-directional CNN-BiLSTM network using EEG signals." IEEE Trans. Neural Syst. Rehabil. Eng., 2020.

[13] S. Crea, M. Nann, E. Trigili, F. Cordella, A. Baldoni, F. J. Badesa, J. M. Catalán, L. Zollo, N. Vitiello, N. G. Aracil, and S. R. Soekadar, "Feasibility and safety of shared EEG/EOG and vision-guided autonomous whole-arm exoskeleton control to perform activities of daily living," Sci. Rep., vol. 8, p. 10823, 2018.

[14] X. Chen, B. Zhao, Y. Wang, S. Xu, and X. Gao, "Control of a 7-DOF robotic arm system with an SSVEP-based BCI," Int. J. Neural Syst., vol. 28, no. 8, p. 1850018, 2018.

[15] J.-H. Jeong, N.-S. Kwak, C. Guan, and S.-W. Lee, "Decoding movement-related cortical potentials based on subject-dependent and section-wise spectral filtering." IEEE Trans. Neural Syst. Rehabil. Eng., vol. 28, no. 3, pp. 687–698, 2020.

[16] D. Kuhner, L. Fiederer, J. Aldinger, F. Burget, M. Völker, R. Schirrmeister, C. Do, J. Boedecker, B. Nebel, T. Ball, and W. Burgard, "A service assistant combining autonomous robotics, flexible goal formulation, and deep-learning-based brain-computer interfacing," Rob. Auton. Syst., vol. 116, pp. 98–113, 2019.

[17] N.-S. Kwak, K.-R. Müller, and S.-W. Lee, "A convolutional neural network for steady state visual evoked potential classification under ambulatory environment," PloS One, vol. 12, no. 2, p. e0172578, 2017.

[18] M. Lee, C.-H. Park, C.-H. Im, J.-H. Kim, G.-H. Kwon, L. Kim, W. H. Chang, and Y.-H. Kim, "Motor imagery learning across a sequence of trials in stroke patients," Restor. Neurol. Neurosci., vol. 34, no. 4, pp. 635–645, 2016.

[19] L. F. Nicolas-Alonso and J. Gomez-Gil, "Brain computer interfaces, a review," Sensors, vol. 12, no. 2, pp. 1211–1279, 2012.

[20] R. Leeb, L. Tonin, M. Rohm, L. Desideri, T. Carlson, and J. d. R. Millán, "Towards independence: A BCI telepresence robot for people with severe motor disabilities," Proc. IEEE, vol. 103, no. 6, pp. 969–982, 2015.

[21] H.-I. Suk and S.-W. Lee, "A novel bayesian framework for discriminative feature extraction in brain-computer interfaces," IEEE Trans. Pattern Anal. Mach. Intell., vol. 35, no. 2, pp. 286–299, 2012.

[22] T.-E. Kam, H.-I. Suk, and S.-W. Lee, "Non-homogeneous spatial filter optimization for electroencephalogram (EEG)-based motor imagery classification," Neurocomputing, vol. 108, pp. 58–68, 2013.

[23] K. K. Ang and C. Guan, "EEG-based strategies to detect motor imagery for control and rehabilitation," IEEE Trans. Neural Syst. Rehabil. Eng., vol. 25, no. 4, pp. 392–401, 2017.

[24] L. Yao, N. Mrachacz-Kersting, X. Sheng, X. Zhu, D. Farina, and N. Jiang, "A multi-class BCI based on somatosensory imagery," IEEE Trans. Neural Syst. Rehabil. Eng., vol. 26, no. 8, pp. 1508–1515, 2018.

[25] X. Yong and C. Menon, "EEG classification of different imaginary movements within the same limb," PLoS One, vol. 10, no. 4, p. e0121896, 2015.

[26] J.-H. Kim, F. Bießmann, and S.-W. Lee, "Decoding three-dimensional trajectory of executed and imagined arm movements from electroencephalogram signals," IEEE Trans. Neural Syst. Rehabil. Eng., vol. 23, no. 5, pp. 867–876, 2015.

[27] A. Schwarz, P. Ofner, J. Pereira, A. I. Sburlea, and G. R. Müller-Putz, "Decoding natural reach-and-grasp actions from human EEG," J. Neural Eng., vol. 15, no. 1, p. 016005, 2017.

[28] F. Galán, M. R. Baker, K. Alter, and S. N. Baker, "Degraded EEG decoding of wrist movements in absence of kinaesthetic feedback," Hum. Brain Mapp., vol. 36, no. 2, pp. 643–654, 2015.

[29] Y. Zhang, C. S. Nam, G. Zhou, J. Jin, X. Wang, and A. Cichocki, "Temporally constrained sparse group spatial patterns for motor imagery BCI," IEEE Trans. on Cybernetics, vol. 49, no. 9, pp. 3322–3332, 2018.

[30] F. Shiman, E. López-Larraz, A. Sarasola-Sanz, N. Irastorza-Landa, M. Spüler, N. Birbaumer, and A. Ramos-Murguialday, "Classification of different reaching movements from the same limb using EEG," J. Neural Eng., vol. 14, no. 4, p. 046018, 2017.

[31] B. J. Edelman, B. Baxter, and B. He, "EEG source imaging enhances the decoding of complex right-hand motor imagery tasks," IEEE Trans. Biomed. Eng., vol. 63, no. 1, pp. 4–14, 2015.

[32] O. W. Samuel, Y. Geng, X. Li, and G. Li, "Towards efficient decoding of multiple classes of motor imagery limb movements based on EEG spectral and time domain descriptors," J. Med. Syst., vol. 41, no. 12, p. 194, 2017.

[33] X. Li, O. W. Samuel, X. Zhang, H. Wang, P. Fang, and G. Li, "A motion-classification strategy based on sEMG-EEG signal combination for upper-limb amputees," J. Neuroeng. Rehabil., vol. 14, no. 1, p. 2, 2017.

[34] A. Úbeda, J. M. Azorín, R. Chavarriaga, and J. d. R. Millán, "Classification of upper limb center-out reaching tasks by means of EEG-based continuous decoding techniques," J. Neuroeng. Rehabil., vol. 14, no. 9, pp. 1–14, 2017.

[35] Y. R. Tabar and U. Halici, "A novel deep learning approach for classification of EEG motor imagery signals," J. Neural Eng., vol. 14, no. 1, p. 016003, 2016.

[36] A. Craik, Y. He, and J. L. P. Contreras-Vidal, "Deep learning for electroencephalogram (EEG) classification tasks: A review," J. Neural Eng., vol. 16, no. 3, p. 031001, 2019.

[37] N. Lu, T. Li, X. Ren, and H. Miao, "A deep learning scheme for motor imagery classification based on restricted Boltzmann machines," IEEE Trans. Neural Syst. Rehabil. Eng., vol. 25, no. 6, pp. 566–576, 2017.

[38] Z. Zhang, F. Duan, J. Solé-Casals, J. Dinarès-Ferran, A. Cichocki, Z. Yang, and Z. Sun, "A novel deep learning approach with data augmentation to classify motor imagery signals," IEEE Access, vol. 7, pp. 15 945–15 954, 2019.

[39] P. Wang, A. Jiang, X. Liu, J. Shang, and L. Zhang, "LSTM-based EEG classification in motor imagery tasks," IEEE Trans. Neural Syst. Rehabil. Eng., vol. 26, no. 11, pp. 2086–2095, 2018.

[40] B. Xu, Z. Wei, A. Song, C. Wu, D. Zhang, W. Li, G. Xu, H. Li, and H. Zeng, "Phase synchronization information for classifying motor imagery EEG from the same limb," IEEE Access, vol. 7, pp. 153 842–153 852, 2019.

[41] P. Wei, W. He, Y. Zhou, and L. Wang, "Performance of motor imagery brain-computer interface based on anodal transcranial direct current stimulation modulation," IEEE Trans. Neural Syst. Rehabil. Eng., vol. 21, no. 3, pp. 404–415, 2013.

[42] J.-H. Jeong, K.-H. Shim, D.-J. Kim, and S.-W. Lee, "Trajectory decoding of arm reaching movement imageries for brain-controlled robot arm system," in Proc. 41th Int. Conf. IEEE Eng. Med. Biol. Soc. (EMBC). Berlin, Germany, July 23 2019, pp. 5544–5547.

[43] S. Sakhavi, C. Guan, and S. Yan, "Learning temporal information for brain-computer interface using convolutional neural networks," IEEE Trans. on Neural Netw. Learn. Syst., vol. 29, no. 11, pp. 5619–5629, 2018.

[44] B. Singh and H. Wagatsuma, "A removal of eye movement and blink artifacts from EEG data using morphological component analysis," Comput. Math. Method M., vol. 2017, 2017.

[45] A. Jafarifarmand, M. A. Badamchizadeh, S. Khanmohammadi, M. A. Nazari, and B. M. Tazehkand, "A new self-regulated neuro-fuzzy framework for classification of EEG signals in motor imagery BCI," IEEE Trans. Fuzzy Syst., vol. 26, no. 3, pp. 1485–1497, 2017.

[46] G. Xu, X. Shen, S. Chen, Y. Zong, C. Zhang, H. Yue, M. Liu, F. Chen, and W. Che, "A deep transfer convolutional neural network framework for EEG signal classification," IEEE Access, vol. 7, pp. 112 767–112 776, 2019.

[47] M. Alhussein, G. Muhammad, and M. S. Hossain, "EEG pathology detection based on deep learning," IEEE Access, vol. 7, pp. 27 781–27 788, 2019.

[48] K. K. Ang, Z. Y. Chin, H. Zhang, and C. Guan, "Filter bank common spatial pattern (FBCSP) in brain-computer interface," in IEEE Int. Joint Conf. on Neural Netw., 2008, pp. 2390–2397.

[49] R. T. Schirrmeister, J. T. Springenberg, L. D. J. Fiederer, M. Glasstetter, K. Eggensperger, M. Tangermann, F. Hutter, W. Burgard, and T. Ball, "Deep learning with convolutional neural networks for EEG decoding and visualization," Hum. Brain Mapp., vol. 38, no. 11, pp. 5391–5420, 2017.

[50] V. J. Lawhern, A. J. Solon, N. R. Waytowich, S. M. Gordon, C. P. Hung, and B. J. Lance, "EEGNet: a compact convolutional neural network for EEG-based brain–computer interfaces," J. Neural Eng., vol. 15, no. 5, p. 056013, 2018.

[51] S. Panchapagesan, M. Sun, A. Khare, S. Matsoukas, A. Mandal, B. Hoffmeister, and S. Vitaladevuni, "Multi-task learning and weighted cross-entropy for DNN-based keyword spotting." in Interspeech, vol. 9, 2016, pp. 760–764.

[52] Z. Zhang, and M. Sabuncu, "Generalized cross entropy loss for training deep neural networks with noisy labels," in Proc. Adv. Neural Inf. Process. Syst. (NIPS), 2018, pp. 8778–8788.

[53] K. K. Ang, Z. Y. Chin, C. Wang, C. Guan, and H. Zhang, "Filter bank common spatial pattern algorithm on BCI competition iv datasets 2a and 2b," Front Neurosci., vol. 6, p. 39, 2012.

[54] P. Ofner, A. Schwarz, J. Pereira, and G. R. Müller-Putz, "Upper limb movements can be decoded from the time-domain of low-frequency EEG," PLoS One, vol. 12, no. 8, p. e0182578, 2017.

[55] B.-H. Lee, J.-H. Jeong, K.-H. Shim, and S.-W. Lee, "Classification of high-dimensional motor imagery tasks based on an end-to-end role assigned convolutional neural network," in in Conf. Proc. IEEE Int. Acoust. Speech Signal Process. (ICASSP), May. 2020.

[56] J.-H. Jeong, B.-W. Yu, D.-H. Lee, and S.-W. Lee, "Classification of drowsiness levels based on a deep spatio-temporal convolutional bidirectional LSTM network using electroencephalography signals," Brain Sci., vol. 9, no. 12, p. 348, 2019.
[57] Z. Jiao, X. Gao, Y. Wang, J. Li, and H. Xu, "Deep convolutional neural networks for mental load classification based on EEG data," Pattern Recognit., vol. 76, pp. 582–595, 2018.
[58] P. Zhang, X. Wang, W. Zhang, and J. Chen, "Learning spatial–spectral–temporal EEG features with recurrent 3D convolutional neural networks for cross-task mental workload assessment," IEEE Trans. Neural Syst. Rehabil. Eng., vol. 27, no. 1, pp. 31–42, 2019.
[59] T. K. Reddy, V. Arora, and L. Behera, "HJB-equation-based optimal learning scheme for neural networks with applications in brain–computer interface," IEEE Trans. Emerg. Topics Comput. Intell., pp. 1–12, 2018.
[60] S. Alhagry, A. A. Fahmy, and R. A. El-Khoribi, "Emotion recognition based on EEG using LSTM recurrent neural network," Emotion, vol. 8, no. 10, pp. 355–358, 2017.
[61] E. S. Salama, R. A. El-Khoribi, M. E. Shoman, and M. A. W. Shalaby, "EEG-based emotion recognition using 3D convolutional neural networks," Int. J. Adv. Comput. Sci. Appl., vol. 9, no. 8, pp. 329–337, 2018.
[62] J. Li, Z. L. Yu, Z. Gu, W. Wu, Y. Li, and L. Jin, "A hybrid network for ERP detection and analysis based on restricted Boltzmann machine," IEEE Trans. Neural Syst. Rehabil. Eng., vol. 26, no. 3, pp. 563–572, 2018.
[63] A. Ditthapron, N. Banluesombatkul, S. Ketrat, E. Chuangsuwanich, and T. Wilaiprasitporn, "Universal joint feature extraction for P300 EEG classification using multi-task autoencoder," IEEE Access, vol. 7, pp. 68 415–68 428, 2019.
[64] H.-I. Suk and S.-W. Lee, "Subject and class specific frequency bands selection for multiclass motor imagery classification," Int. J. Imaging Syst. Technol., vol. 21, no. 2, pp. 123–130, 2011.
[65] O.-Y. Kwon, M.-H. Lee, C. Guan, and S.-W. Lee, "Subject-independent brain-computer interfaces based on deep convolutional neural networks," IEEE Trans. Neural Netw. Learn. Syst., pp. 1–14, 2019.
[66] A. Singh, S. Lal, and H. W. Guesgen, "Reduce calibration time in motor imagery using spatially regularized symmetric positives-definite matrices based classification," Sensors, vol. 19, no. 2, p. 379, 2019.

JI-HOON JEONG received his B.S. degree in computer information science from Korea University, South Korea, in 2015. He is an integrated master-Ph.D. student in the Department of Brain and Cognitive Engineering at Korea University, South Korea. His research interests include deep learning, brain-computer interfaces, and human-machine intelligence.

BYEONG-HOO LEE received his B.S. degree in electronic engineering from Hanyang University, South Korea, in 2019. He is a master student in the Department of Brain and Cognitive Engineering at Korea University, South Korea. His research interests include deep learning, brain-computer interfaces, signal processing.

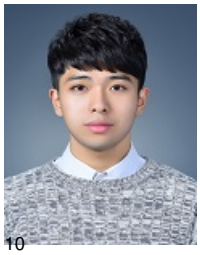

DAE-HYEOK LEE revceived his B.S. degree in bioengineering from UNIST, South Korea, in 2018. He is a master student in the Department of Brain and Cognitive Engineering at Korea University, South Korea. His research interests include signal processing, deep learning, and brain-computer interface.

YONG-DEOK YUN received his B.S. degree in mechanical and information engineering from University of Seoul, South Korea, in 2017. He received his M.S. degree in brain and cognitive engineering from Korea University, South Korea, in 2019. His research interests include machine learning and brain-machine interface.

SEONG-WHAN LEE (S'84–M'89–SM'96–F'10) received the B.S. degree in computer science and statistics from Seoul National University, South Korea, in 1984, and the M.S. and Ph.D. degrees in computer science from the Korea Advanced Institute of Science and Technology, South Korea, in 1986 and 1989, respectively. He is currently the head of the Department of Artificial Intelligence, Korea University, Seoul. His current research interests include artificial intelligence, pattern recognition, and brain engineering. Dr. Lee is a fellow of the International Association of Pattern Recognition (IAPR) and the Korea Academy of Science and Technology.